JOURNAL OF GEOPHYSICAL RESEARCH, VOL. 111, G03008, doi:10.1029/2006JG000166, 2006

Click Here for Full Article

A forward modeling approach to paleoclimatic interpretation of tree-ring data

M. N. Evans,[1,2,3] B. K. Reichert,[4,5] A. Kaplan,[4] K. J. Anchukaitis,[1,2] E. A. Vaganov,[6] M. K. Hughes,[1] and M. A. Cane[4]

Received 17 January 2006; accepted 24 May 2006; published 10 August 2006.

[1] We investigate the interpretation of tree-ring data using the Vaganov-Shashkin forward model of tree-ring formation. This model is derived from principles of conifer wood growth, and explicitly incorporates a nonlinear daily timescale model of the multivariate environmental controls on tree-ring growth. The model results are shown to be robust with respect to primary moisture and temperature parameter choices. When applied to the simulation of tree-ring widths from North America and Russia from the Mann et al. (1998) and Vaganov et al. (2006) data sets, the forward model produces skill on annual and decadal timescales which is about the same as that achieved using classical dendrochronological statistical modeling techniques. The forward model achieves this without site-by-site tuning as is performed in statistical modeling. The results support the interpretation of this broad-scale network of tree-ring width chronologies primarily as climate proxies for use in statistical paleoclimatic field reconstructions, and point to further applications in climate science.

Citation: Evans, M. N., B. K. Reichert, A. Kaplan, K. J. Anchukaitis, E. A. Vaganov, M. K. Hughes, and M. A. Cane (2006), A forward modeling approach to paleoclimatic interpretation of tree-ring data, *J. Geophys. Res.*, *111*, G03008, doi:10.1029/2006JG000166.

1. Introduction

[2] A key element of climate change detection and attribution efforts is the determination of natural variability on timescales bracketing those of anthropogenic influences on climate. In the absence of direct observations, especially prior to the rise of globally distributed direct observations in the mid 19th century, we rely on the so-called "proxy" climate indicators, which are often derived from geological or biological archives, and are interpreted by means of statistical relationships and chemical or biophysical principles. One of the most widespread kinds of natural paleoclimatic archives are tree rings; data now exist from over 2000 sites on six continents [*World Data Center for Paleoclimatology*, 2003]. The collection and interpretation of these data sets is based in biological principles of tree growth [e.g., *Schweingruber*, 1988; *Cook and Kairiukstis*, 1990; *Fritts*, 1991]. Subsequent analysis of derived paleoclimate observational networks incorporating tree-ring records and other proxy data has produced hemispheric and global-scale paleoclimatic reconstructions over the past few centuries to millennia [e.g., *Mann et al.*, 1998, 1999; *Stahle et al.*, 1998; *Briffa et al.*, 2001; *Jones et al.*, 2001; *Esper et al.*, 2002; *Cook et al.*, 2002; *Mann and Jones*, 2003].

[3] Two major uncertainties lie in the statistical development, analysis and interpretation of tree-ring data for paleoclimate studies. First, there are nonclimatic influences on tree-ring records, including tree biology, size, age and the effects of localized forest dynamics [*Cook and Kairiukstis*, 1990]. Successful elimination of these influences is now routinely achieved via careful site selection, sampling, data analysis and a posteriori tests to ensure that the tree-ring record is dominated by the single climate variable of interest. Perhaps of more concern is that tree-ring data reflect a nonlinear response to multivariate climate forcings. This represents a problem for both single-variable paleoclimatic reconstructions via linear statistical calibration of the tree-ring proxy data and for prediction of the effects of climate change scenarios on tree biology and forest ecology. In both situations, statistical relationships, which may represent linearizations of nonlinear processes (see section 2), are difficult to validate for long period processes and for times outside the instrumental era and may not hold for paleoclimate or climate change experiments. For example, the application of statistical calibrations to an independent time period with a fundamentally different climatic regime, for example, with comparable temperatures but a general shift in water balance, may

[1] Laboratory of Tree-Ring Research, University of Arizona, Tucson, Arizona, USA.
[2] Also at Department of Geosciences, University of Arizona, Tucson, Arizona, USA.
[3] Also at Lamont-Doherty Earth Observatory, Columbia University, Palisades, New York, USA.
[4] Lamont-Doherty Earth Observatory, Columbia University, Palisades, New York, USA.
[5] Now at German Meteorological Service, Offenbach, Germany.
[6] V. N. Sukachev Institute of Forest, Russian Academy of Sciences, Krasnoyarsk, Russia.

Copyright 2006 by the American Geophysical Union.
0148-0227/06/2006JG000166$09.00

consequently lead to an erroneous climate reconstruction [*LaMarche et al.*, 1984; *Graybill and Idso*, 1993; *Briffa et al.*, 1998; *Vaganov et al.*, 1999; *Barber et al.*, 2000; *Kirdyanov et al.*, 2003; *Anchukaitis et al.*, 2006]. Hence the nature of trees as a biological archive of environmental conditions raises questions about the validity of linear, statistical approaches to interpretation of the data.

[4] Introduction of a process model of tree-ring growth, from which tree ring formation is represented via first principles of tree biology and climate data, permits us to investigate these issues directly. Here we investigate the potential of the Vaganov-Shashkin model of tree-ring formation [*Shashkin and Vaganov*, 1993; *Vaganov et al.*, 1990, 2006] (see also E. A. Vaganov et al., How well understood are the processes that create dendroclimatic records? A mechanistic model of climatic control on conifer tree-ring growth dynamics, submitted to *Dendroclimatology: Progress and Prospects*, edited by M. K. Hughes, T. W. Swetnam, and H. F. Diaz, Springer, 2006) (hereinafter referred to as Vaganov et al., submitted manuscript, 2006) to accurately simulate trees growing in a variety of environmental conditions. Although there are several other process models of tree growth and ring formation [e.g., *Fritts et al.*, 1999; *Foster and LeBlanc*, 1993; *Misson*, 2004], our interest in a robust if low-order forward model with a prognostic variable directly comparable to standard proxy observations led us to work with the Vaganov-Shashkin model. The tree-ring process model is briefly reviewed in section 2. A more comprehensive description of the development, theory, and justification of model components has recently been published by *Vaganov et al.* [2006, submitted manuscript, 2006]; the reader is referred to this monograph for more details. This study, however, is a report of the first broad-scale application of this model to the simulation of tree-ring width data used for statistical paleoclimatology. The model is applied to the simulation of the actual tree-ring chronology data described in section 3. Performance of the model is reported in section 4. The implications of the results are discussed in section 5; conclusions are summarized in section 6.

2. Model Description

2.1. General Principles

[5] The Vaganov-Shashkin model has two distinguishing features. First, it deals with rates of growth of cells as if their formation in the cambium is influenced exclusively by the physical environment. This is a major simplification of present knowledge of wood biology, made for the purpose of simplifying the model and reducing the number of parameters. Second, it deals explicitly with the dynamics of cell growth, division, and maturation in a dedicated "cambial block" that is described briefly here and in detail elsewhere [*Vaganov et al.*, 2006, submitted manuscript, 2006]. This cambial block is driven by and is connected with the growth block. Thus the model simulates not only the width of conifer tree rings but also aspects of their internal structure, reflecting intraseasonal environmental fluctuations.

[6] The growth block of the Vaganov-Shashkin tree-ring model uses the principle of limiting factors [e.g., *Fritts*, 1991] to calculate conifer tree-ring formation integrated over the growing season from daily temperature, precipitation, and sunlight. The daily growth rate on a specific day t is modeled as

$$G(t) = g_E(t)\min[g_T(t), g_W(t)],$$

where $g_E(t)$, $g_T(t)$, and $g_W(t)$ are the daily growth rates due to solar radiation, near-surface air temperature, and soil water balance, respectively. Dependence of growth on solar radiation $g_E(t)$ is a function of latitude, declination angle and hour angle [*Gates*, 1980, equation (6.10)]; any reduction of g_E by canopy shading has been neglected. The effects of the eccentricity of the Earth's orbit around the Sun and of atmospheric transmissivity have been neglected. The minimum function permits tree-ring formation to vary in effective functional dependence among temperature, moisture and sunlight on daily through seasonal timescales. Below, we briefly describe the component functions contributing to $G(t)$, as well as the environmentally driven cambial model. Much more detail on the VS model is found in the literature [*Vaganov et al.*, 1990, 1994; *Vaganov*, 1996; *Vaganov et al.*, 1999, 2000]; a comprehensive review of its development and application is given by *Vaganov et al.* [2006, submitted manuscript, 2006]. A schematic overview of the model, its inputs and prognostics is given in Figure 1. Model parameters not varying in time, their assumed values and units are given in Table 1. These values were determined from the literature and from intensive case studies at a limited number of sites [*Vaganov et al.*, 2006, chap. 7] (see also section 4.2 of this paper).

2.2. Growth Response to Temperature

[7] Experimental data [*Fritts*, 1976; *Kramer and Kozlowski*, 1979; *Gates*, 1980; *Lyr et al.*, 1992] suggest that the dependence of the growth rate function on temperature g_T may be subdivided into three segments: (1) rising growth rates with increasing temperatures below a growth-optimal temperature range; (2) relatively constant rates within an optimal range of temperatures; and (3) decreasing growth rates above that temperature range. This also represents the typical behavior of other biological systems. A polynomial function has been suggested [*Vaganov et al.*, 1990; *Fritts*, 1991] which is approximated in the Vaganov-Shashkin model by a piecewise linear function (Figure 1). Between the minimum temperature for growth $T_{\min}$ and the lower end of the range of optimal temperatures T_{opt1}, the growth rate linearly increases with temperature. Between T_{opt1} and T_{opt2}, growth rate is optimal at a constant level, then decreasing linearly between T_{opt2} and the maximum temperature for growth $T_{\max}$. Beyond $T_{\max}$, growth does not occur. Following studies by *Lindsay and Newman* [1956], *Landsberg* [1974], *Valentine* [1983], *Cannell and Smith* [1986], and *Hanninen* [1991], growth in the model's representation of cambial processes (see section 2.4) is initiated each year when the sum of daily temperatures over a specified time period t_{beg} reaches a defined critical level T_{beg} (Table 1).

2.3. Growth Response to Water Balance

[8] Similar to calculation of growth response to temperature $g_T(t)$, growth response to soil water balance $g_W(t)$ is also expressed as a piecewise-linear function of W (Figure 1), which represents another approximation based

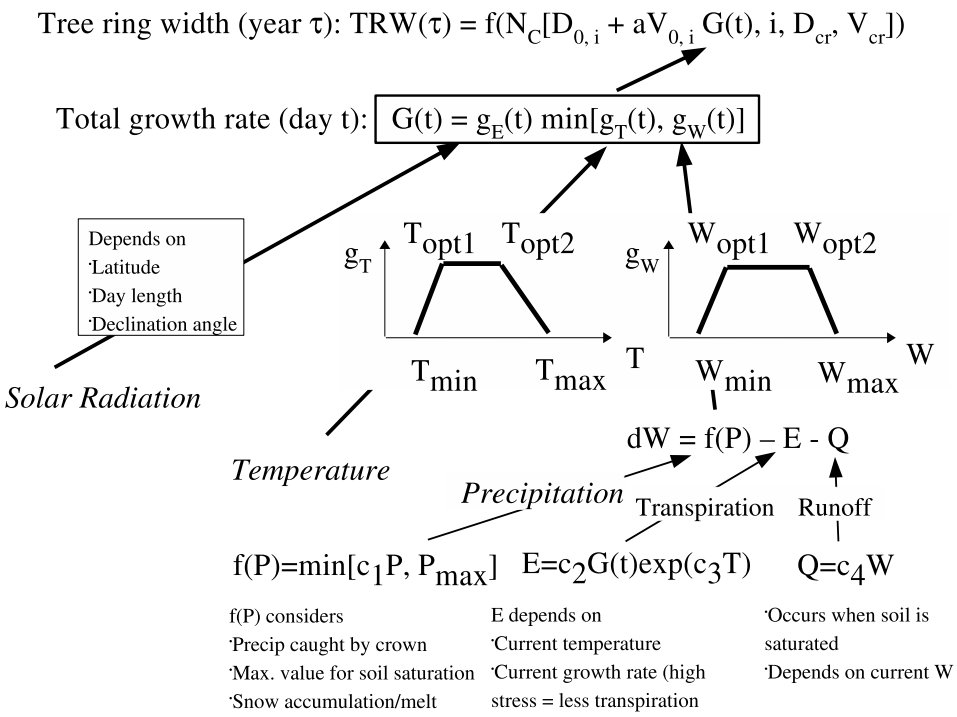

Figure 1. Schematic representation of the Vaganov-Shashkin tree-ring model (see section 2). Daily model inputs (solar radiation, temperature, and precipitation) are italicized.

on experimental data [*Kramer and Kozlowski*, 1979]. The soil water content W itself is calculated through a balance equation for soil water dynamics [*Thornthwaite and Mather*, 1955; *Alisov*, 1956],

$$dW = f(P) - E - Q.$$

Here dW is the daily change in soil water content, $f(P)$ is a function of daily precipitation, E is daily transpiration, and Q denotes daily runoff. Function $f(P)$ is expressed as

$$f(P) = \min\left[c_1 P, P_{\max}\right],$$

where P is the actual daily precipitation, the constant c_1 is the fraction of precipitation that is caught by the crown of the tree, and $P_{\max}$ denotes the maximum level for saturated soil. In the case of temperatures near freezing, P is modified to allow for snow melt (if temperatures are above freezing and snow is present from prior-day calculations) or snow accumulation (if temperatures are below freezing and precipitation has occurred that day). For saturated soil, runoff Q is proportional to the soil water content W,

$$Q = \Lambda W.$$

Table 1. Tree-Ring Model Parameters Used Throughout This Study

Parameter	Description (Units)	Value
$T_{\min}$	minimum temperature for tree growth (°C)	5.0
T_{opt1}	lower end of range of optimal temperatures (°C)	18.0
T_{opt2}	upper end of range of optimal temperatures (°C)	24.0
$T_{\max}$	maximum temperature for tree growth (°C)	31.0
$W_{\min}$	minimum soil moisture for tree growth, relative to saturated soil (v/vs)	0.04
W_{opt1}	lower end of range of optimal soil moistures (v/vs)	0.2
W_{opt2}	upper end of range of optimal soil moistures (v/vs)	0.8
$W_{\max}$	maximum soil moisture for tree growth (v/vs)	0.9
T_{beg}	temperature sum for initiation of growth (° C)	60
t_{beg}	time period for temperature sum (days)	10
l_r	depth of root system (mm)	1000
$P_{\max}$	maximum daily precip. for saturated soil (mm/day)	20
c_1	fraction of precipitation penetrating soil (not caught by crown) (rel. unit)	0.72
c_2	first coefficient for calculation of transpiration (mm/day)	0.12
c_3	second coefficient for calculation of transpiration (1/°C)	0.175
Λ	coefficient for water drainage from soil (dimensionless)	0.001
t_c	cambial model time step (days)	0.2
V_{cr}	minimum cambial cell growth rate (μm/day)	0.04
D_o	initial cambial cell size (μm)	4
D_{cr}	cell size at which mitotic cycle begins (μm)	8
V_m	growth rate during mitotic cycle (μm/day)	1
D_m	cambial cell size at which mitosis occurs (μm)	10

The transpiration of water by the tree crown E depends exponentially on temperature [*Monteith and Unsworth*, 1990] and linearly on the growth function G,

$$E = c_2 G(t) \exp[c_3 T],$$

where the constants c_2 and c_3 are used to describe a variety of tree species and growth conditions (Table 1). The factor $c_2G(t)$ is related to stomatal conductance. In practice, the dependence of E on T is strongly constrained by the functional forms of G, g_T and g_W (Figure 1 and Table 1; results not shown). For example, while a temperature increase into the range $T_{opt1} - T_{opt2}$ will increase g_T, a concurrent temperature-driven increase in evapotranspiration will reduce soil moisture. The latter effect decreases W, and if W falls outside the range $W_{opt1} - W_{opt2}$, leads to limitation of E by g_W, via G.

2.4. Cambial Model

[9] In the component of the model which simulates the growth and formation of wood cells in the tree cambium, the daily growth rate is used to calculate the cellular growth rate $V_i(t)$,

$$V_i(t) = V_{0,i} G(t),$$

where the index i indicates the position in the cambial zone of the growing cell, and $V_{0,i}$ is the linear dependence of growth rate on position. Each cell is permitted to be dormant, grow, divide and/or differentiate into xylem on an intraday time interval t_c. If the cell is not large enough to divide, and if $V_i(t)$ is below a constant critical level V_{cr}, the cell is considered dormant and does not grow, divide or differentiate. If the cellular growth rate is greater than V_{cr} but is less than a position-dependent minimum growth rate $V_{\min}$ [*Fritts et al.*, 1999], then the cell can no longer divide, and exits the cambial zone. Otherwise, the cell grows from an initial size D_o according to the environmentally scaled growth rate $V_i(t)$ for that intraday interval. If the cell reaches or exceeds a critical cambial cell size D_{cr}, the cell must enter and complete the mitotic cycle. The cell now grows at an environmentally independent and constant growth rate V_m until it reaches division size D_m. At this point, it is divided into two adjacent cells, each equal in size to one half of the parent cell size. At the end of the growing season ($G \rightarrow 0$), growth rate of the remaining cells in the cambial zone fall below V_{cr} and become dormant. They now represent the initial cambial cells for the subsequent growing season.

[10] In nature, tree-ring width (*TRW*) is determined by the sum of the radial cell sizes of all cells produced during the growing season. In the version of the model that we used for this study, however, *TRW* is estimated via the normalized number of noncambial cells N formed that year through the aforementioned processes of growth, division and differentiation (Figure 1, top two lines). This is possible because there is always a strong linear relationship between N and *TRW* [*Gregory*, 1971; *Vaganov et al.*, 1985; *Camerero et al.*, 1998; *Wang et al.*, 2002; *Vaganov et al.*, 2006, submitted manuscript, 2006]. Hence, in the model simulation,

$$TRW(\tau) = \frac{N}{\langle N \rangle_\tau},$$

where τ is now time interval in units of annual growing seasons, and $\langle \ldots \rangle_\tau$ indicates the time average over the entire simulation. The simulated standardized (dimensionless) tree-ring width chronologies may then be directly compared to actual standardized tree-ring width data.

2.5. Model Operationalization

[11] The Vaganov-Shashkin model is integrated in the following manner.

[12] 1. The overall growth function G is calculated on the basis of current g_E, g_T and g_W. Here g_E depends on latitude and time; g_T depends on current-day T; g_W depends on an initial or prior-day W and dW, which in turn are based on precipitation, soil drainage, and snowmelt or accumulation.

[13] 2. The cambial growth rate $V_i(G)$ is calculated for each cambial cell left at the end of the prior growing season, or for each cambial cell from the prior day's calculation. In all simulations described here, the cambial model time step was 1/5 day. Depending on the value of $V_i(G)$ relative to V_{cr} and $V_{\min}$, each cell goes dormant, grows, differentiates into xylem, or divides at each cambial time step.

[14] 3. On the basis of the precipitation function $f(P)$, calculated E, T, and the growth function G, the change in soil moisture $dW = f(P) - E - Q$ is calculated. $W(t + 1) = W(t) + dW(t)$ is calculated for use in the following day's simulation.

[15] 4. The model continues for the following day of the year. At the end of the year τ, *TRW* is calculated from the number of noncambial cells produced over the course of the growing season. The number and size of each cambial cell is used as input for the following year's simulation. At the end of the simulation time interval, *TRW* is normalized by the mean *TRW* for all years of the simulation.

3. Data and Methods

3.1. Tree-Ring Chronologies

[16] At present, there are over 2000 tree-ring chronologies potentially available for intercomparison with synthetic chronologies produced by the tree-ring model [*World Data Center for Paleoclimatology*, 2003; *Contributors of the International Tree Ring Data Bank*, 2002]. However, some of these chronologies were developed for purposes other than paleoclimatic reconstruction, others lack sufficient replication, and yet others were standardized in ways which might limit paleoclimatic interpretation of the data. Hence we selected 198 tree-ring width chronologies for comparison with the tree-ring model output from two sources. All represent site averages of multiple raw ring width series ("chronologies") dated to the calendar year and statistically filtered by the data developers [*Contributors of the International Tree Ring Data Bank*, 2002] to remove purely age dependent time series features. Of these, 190 data series for North America are from the *Mann et al.* [1998] data set. These data were screened a priori for several quality control variables [*Mann et al.*, 2000] to produce a data set most conducive to paleoclimate reconstruction, and represent an excellent target for this study. Data from eight sites in Russia are from published or unpublished data sets developed by *Vaganov et al.* [1999, 2006, submitted manuscript, 2006].

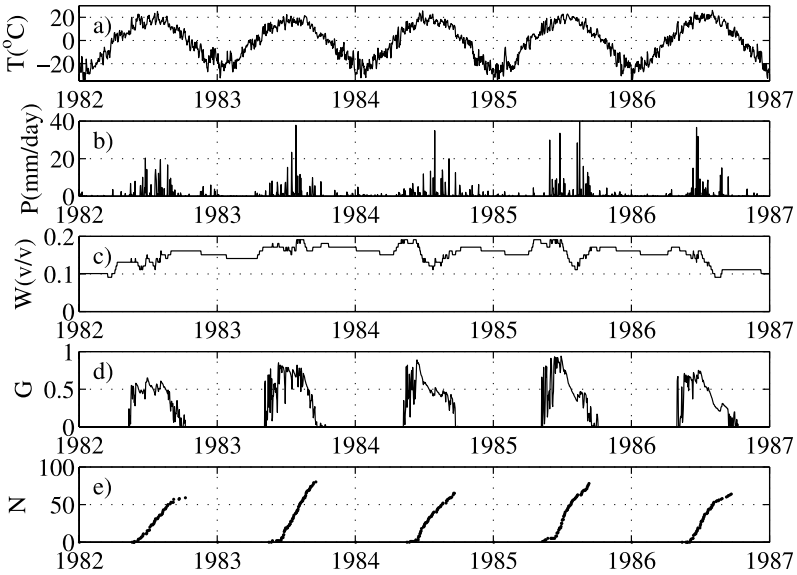

Figure 2. Seasonal soil moisture and temperature controls on simulated tree-ring growth at Ulan-Ude, southern Siberia, 1982–1986. (a, b) Daily temperature T (°C) and precipitation P (mm/day) used to drive the model. (c) Soil moisture W calculated by the water balance component of the model (volume/volume ratio). (d) Annual dimensionless growth response function $G(t)$. (e) Cumulative number of tracheids (wood cells) N per ring for each year's growing season.

3.2. Tree-Ring Width Simulations

[17] Daily station records from the comprehensive Global Historical Climatology Network [*Peterson and Vose*, 1997] data set are used to simulate tree-ring chronologies at North American locations. Daily weather station data for Russian chronology locations is obtained by the Institute of Forest of the Russian Academy of Sciences, Krasnoyarsk, Russia (V. Shishov, personal communication, 2005). Missing temperature data are replaced by linearly interpolated values. Missing precipitation data were simply set to zero. In the case of more than 90 days of missing meteorological data, the year was not simulated. To account for model equilibration, all model simulations were initialized with the same default number of cambial cells and sizes, and initial soil moisture values, and the first modeled year's growth was discarded. The simulated growth following a missing meteorological year was initialized using the last simulated year's initialization file, and the first year following a meteorological hiatus was discarded as well.

[18] We note that meteorological station proximity may not always be the best criterion for selecting the appropriate tree-ring model input. For example, the presence of orography produces spatially isentropic features into patterns of temperature and rainfall on daily to seasonal timescales, and elevation differences between tree-ring sites and meteorological stations may artificially create large differences between actual and simulated chronologies. For these reasons, we attempt to partially correct temperature for elevational differences by using an adiabatic correction (6.6°C/km; [*Wallace and Hobbs*, 1977]) for the mean elevation difference between our set of actual tree-ring chronologies and the meteorological stations. On average, chronologies are located 700 m higher than stations; thus the mean temperature correction of 4.6°C was used for all North American simulations. We then simulated the 190 North American tree-ring width chronologies for all meteorological stations found within a 500-km search radius, and the eight Russian chronologies using meteorological data from the nearest station [*Vaganov et al.*, 2006, submitted manuscript, 2006]. In reporting results for each of the 190 North American sites, we use the simulation for the station found within the 500-km search radius that is most significantly correlated with the given actual tree ring width data series over the full intercomparison period available. This period averaged 1915–1981. For the eight Russian sites the meteorological station data coverage is sparser, and we report the same statistic but for correlation with the closest meteorological station, and without a mean temperature correction.

[19] It is also important to note the rather simplistic approach taken with this application of the process model. The model itself is only a very simple depiction of tree growth [*Vaganov et al.*, 2006, submitted manuscript, 2006]. For example, the model does not explicitly include photosynthesis, and it does not include other possibly important controls on tree growth, such as atmospheric attenuation of solar radiation, nutrient availability, CO_2 fertilization, long-term dependence of tree-ring width on tree age, or anthropogenic influences on growth conditions, except as mirrored in meteorological station temperature and precipitation. In addition we did not tune the model fixed parameters by region, mean climate, or species; all model runs use the parameter values listed in Table 1. However, precisely owing to the simplicity of the model and experimental conditions, we can test, in the sense of Occam's razor, the hypothesis that observed tree-ring variations are due solely to meteorological controls, as represented in the Vaganov-Shashkin model. The same assumption implicitly

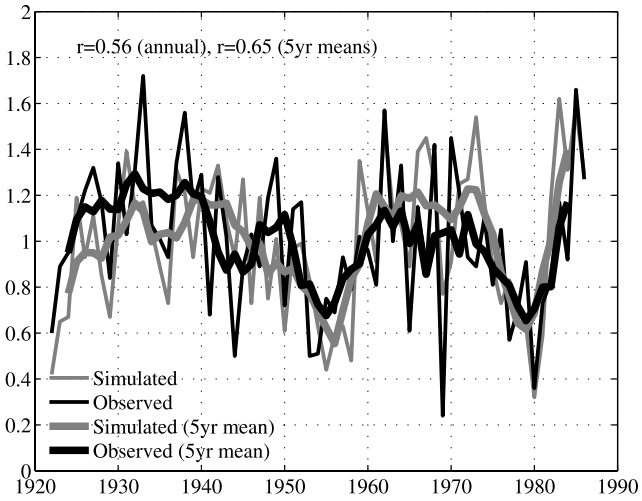

Figure 3. Observed and simulated tree-ring width indices, Ulan-Ude, 1922–1986. Annual (thin lines) and 5-year mean (thick lines) correlations are r = 0.58 and r = 0.65, respectively, both significant at the 99% level for the effective numbers of degrees of freedom.

underlies many uses of tree-ring data in paleoclimate reconstructions.

4. Results

4.1. Model Behavior: Ulan-Ude, Southern Russia

[20] Figure 2 illustrates a single time series ring width simulation (Ulan-Ude, Buryatia region, southern Siberia: 51.8°N, 107.6°E; 510 m elevation) in terms of the intra-annual contributions of the temperature and moisture growth functions for a recent 5-year interval. The model's simulation of annual ring widths is compared to data from a Scots pine (*Pinus sylvestris L.*) tree-ring width chronology [*Andreev et al.*, 1999] from the same region for the period 1922–1989 (Figure 3).

[21] Tree growth for this site is expected to be mainly sensitive to the availability of water, although for specific time periods temperature can become an important factor. In 1985, the beginning of the growth season (which the model defines as when the temperature sum over the period t_{beg} = 10 days has reached the critical level of 60°C (Table 1) is in May (Figure 2). The growth function remains high until the end of June, due to net positive precipitation-evaporation in May and June. A relatively dry period is observed from early July until the end of August. The consequence is a net decrease in available water during that period, resulting in a drastic decrease of the growth function. Although greater precipitation is received in the fall, the growth function is subsequently limited by temperature as the growing season draws to a close. The resulting ring width over the year can, as a first approximation, be seen as the integration over the growth function and shows a relatively wide ring for this year, mainly due to favorable growing conditions until the end of June. By contrast, 1987 shows much lower precipitation within the growth season window defined by the annual cycle of temperature. Consequently, soil moisture was lower throughout the growing season, and the integrated growth function indicates a much narrower predicted tree ring.

[22] The observed and simulated annual tree-ring indices for the available intercomparison period 1922–1986, together with their 5-year running means, are shown in Figure 3. The correlation coefficients for annual data and 5-year averages are $r = 0.58$ and $r = 0.65$, respectively; both correlations are significant at the 99% level. The simulated index for the first year, 1922, does not agree with the observation due to the arbitrariness of model initialization. For other years, the agreement is generally good, with the exception of the years 1933, 1941, 1944, and 1969. The misfit to the tree-ring chronology, especially in 1969, generally coincides with periods when large amounts of daily weather data are missing.

4.2. Model Sensitivity: Ulan-Ude, Southern Russia

[23] To evaluate the sensitivity of the Ulan-Ude results to model parameters which define the temperature and water balance growth functions (Figure 1), we performed two additional experiments (Figure 4). For the first experiment, we varied one of the parameters T_{min}, T_{opt1}, T_{opt2}, and T_{max}, keeping all other parameters constant. The value of each of the varied four parameters (Table 1) was increased and decreased stepwise (steps of ±0.5°C) up to a change of ±5°C, and the simulations were repeated for each new parameter set, resulting in a total of 80 simulated chronologies, which could then be compared to the actual tree-ring chronology from Ulan-Ude. Similarly, the values for W_{min}, W_{opt1}, W_{opt2}, and W_{max} were varied over a range of ±20% and the simulated chronologies compared to the actual chronology.

[24] We found that the tree-ring width simulation for Ulan-Ude was not very sensitive to the choice of primary temperature and water budget parameters (Figures 2 and 4). Decreasing the parameters T_{min} and T_{opt1} have virtually no effect on the simulation; an increase in any of these parameters results in slightly lower but not significantly different correlation coefficients (Figure 4a). Only a decrease of T_{opt2} and T_{max} result in significantly lower correlations, suggesting that lower values for the upper branch of the temperature growth function are unrealistic, consistent with experimental data [e.g., *Gates*, 1980; *Lyr et al.*, 1992]. The second experiment examined the response to variation of the water balance parameters W_{min}, W_{opt1}, W_{opt2}, and W_{max} in the same manner, to ±20% of their original values (Table 1). As W_{opt2} and W_{max} are varied, correlations remain at a constant level for all experiments (Figure 4b), indicating that the soil water balance does not approach a level of saturation that would negatively affect tree ring growth at this site at any time. The important parameters affecting model output here are W_{min} and W_{opt1}. Increasing the values for W_{opt1} does not have a significant influence, whereas increasing W_{min} (the lowest soil water level for the occurrence of growth) seems to have an optimum around the original value. A decrease of either parameter by 20% results in a drop of the correlation coefficient from roughly 0.6 to about 0.3, demonstrating the sensitivity of the model to the lower part of the water balance growth function (Figure 2b). This is consistent with the presumption that tree-ring growth of the investigated chronology is mainly limited by the availability of water.

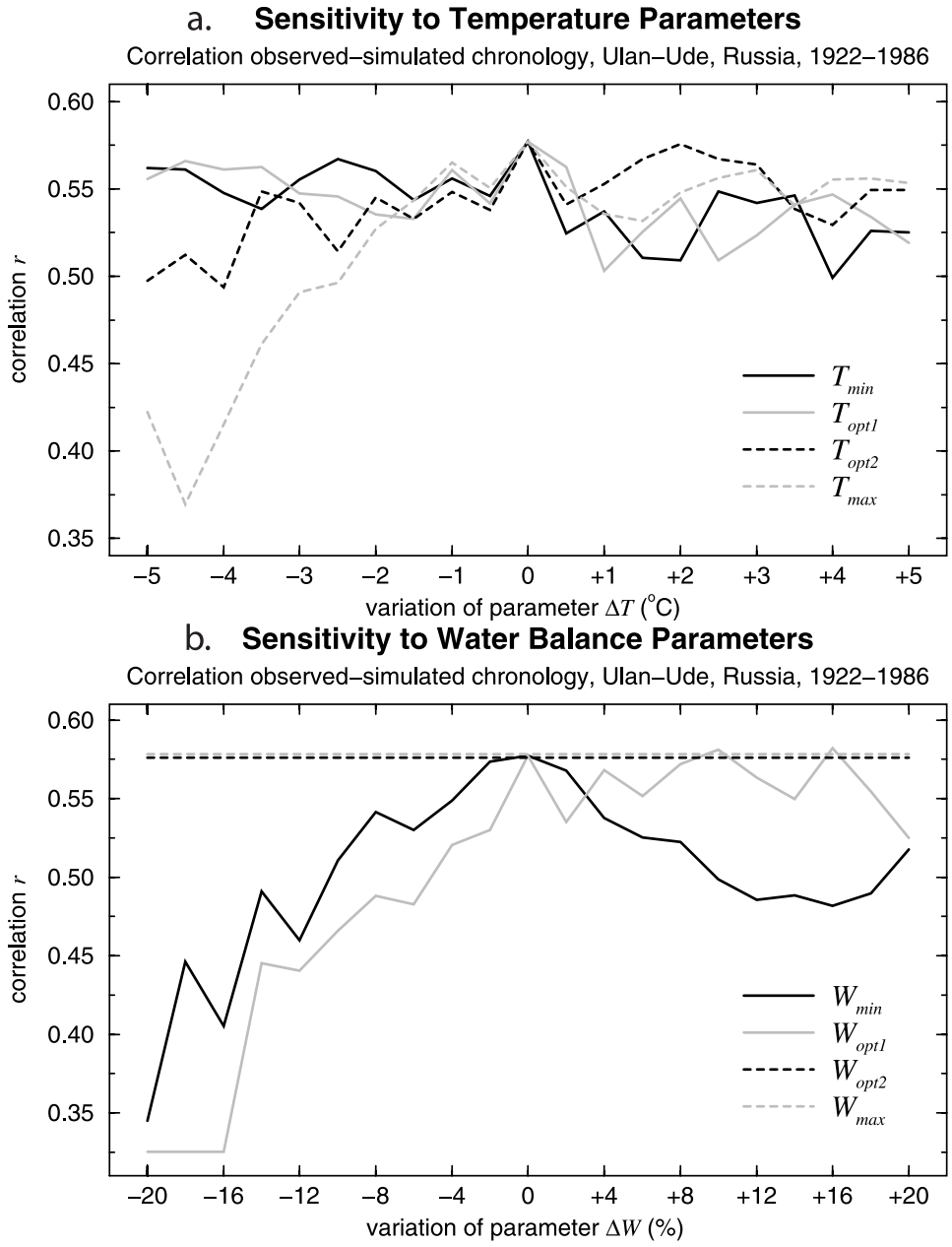

Figure 4. Sensitivity of model simulation to temperature and water balance to parameter choices, Ulan-Ude, 1922–1986. (a) Sensitivity of the correlation between simulated and real tree-ring width chronology as a function of the four temperature parameters T_{min}, T_{opt1}, T_{opt2}, and T_{max}. (b) Sensitivity of the correlation between simulated and real tree-ring width chronology as a function of the four precipitation parameters W_{min}, W_{opt1}, W_{opt2}, and W_{max}.

Table 2. Correlations With North American Chronologies: Process Model Results[a]

Significance Level	Annual Averages ~1915–1981	First Epoch ~1915–1959	Second Epoch ~1960–1981	Decadal ~1915–1981
All	0.47(190)	0.46(190)	0.43(190)	0.61(190)
$p < 0.10$	0.48(176)	0.51(155)	0.58(111)	0.75(65)
$p < 0.05$	0.49(170)	0.53(138)	0.61(84)	0.79(42)
$p < 0.01$	0.51(134)	0.55(107)	0.66(46)	0.85(9)
$p < 0.001$	0.53(101)	0.59(68)	0.70(19)	–(0)

[a]Numbers in parentheses indicate number of averaged correlations.

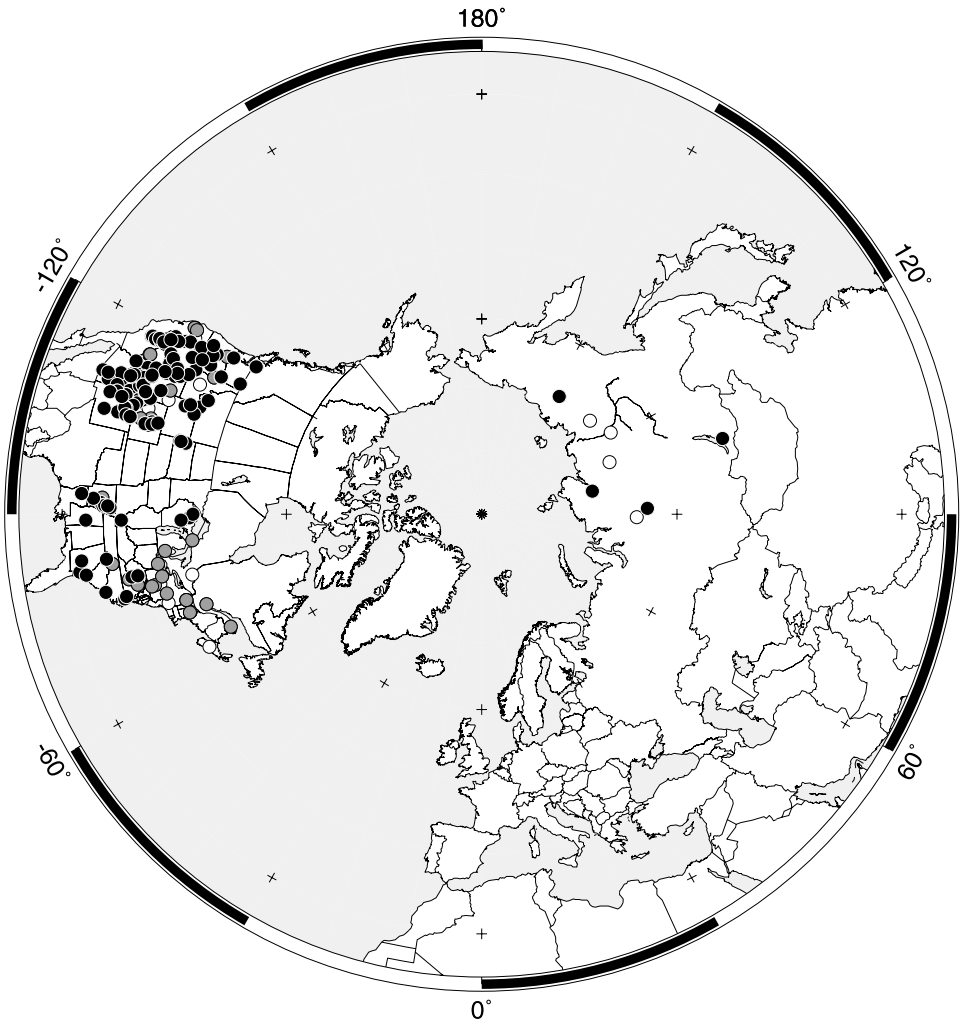

Figure 5. Correlation significance map for simulation of 198 tree ring width chronologies from North America and Russia for the ~1915–1981 comparison period. Significance levels (considering effective degrees of freedom): >99% (black circles; n = 138; 70% of correlations), >95% (gray circles; n = 174; 88% of correlations), <95% (white circles; n = 24; 12% of correlations).

4.3. Simulation of Actual Ring Width Chronologies

[25] A third set of results demonstrates generalized model behavior, as represented by the quality of simulation of the entire set of 198 chronologies described in section 2. We calculate the significance of correlations between all simulated and actual chronologies on annual and decadal (11-year running mean) timescales (Table 2 and Figure 5), taking into account the reduction in effective degrees of freedom due to autocorrelation and temporal averaging [*Trenberth*, 1984; *Donaldson and Tryon*, 1987]; for each chronology, we report the process model correlation having the highest significance within the 500-km search radius over the full intercomparison period. Figure 5 shows the map of the significance of correlations between the 198 simulated and real tree ring chronology data series. A good fit is found across the entire data set, which includes chronologies from the arid western United States, Siberia as well as from the humid, warm eastern United States, and several different species of trees. Table 2 shows the correlation of the 190 North American simulated chronologies on annual and decadal timescales, and for the two epochs (1915–1959 and 1960–1981) of the average common 1915–1981 intercomparison timeframe. The average correlation for all stations over the full period is 0.47. 176 of 190 annual-scale correlations between process-modeled and observed tree-ring width chronologies are significant at the 95% confidence level, with an average correlation of 0.49. Furthermore, the annual correlations are stable with respect to the two chosen epochs (Table 2): The correlation averages are 0.46 and 0.43 in each of these periods. On decadal timescales, the average correlation is 0.61 for all modeled chronologies, the average of the 42 of 190 correlations significant at the 95% confidence level is 0.79.

4.4. Skill Intercomparison: Process and Statistical Modeling

[26] A fourth set of results allows us to assess the process model skill relative to that of multivariate linear statistical models developed using a standard dendroclimatological approach [e.g., *Guiot*, 1990; *Fritts*, 1991; *Cook et al.*, 1999]. For each of the prewhitened 190 North American chronology data series, for all sites within the same 500-km

Table 3. Correlations With North American Chronologies: Statistical Model Results[a]

Significance Level	Annual Averages ~1917–1981	First Epoch ~1917–1960	Second Epoch ~1961–1981	Decadal ~1917–1981
All	0.55(184)	0.60(184)	0.37(184)	0.67(184)
$p < 0.10$	0.55(183)	0.61(181)	0.55(76)	0.75(94)
$p < 0.05$	0.55(181)	0.61(178)	0.59(61)	0.80(56)
$p < 0.01$	0.56(170)	0.62(167)	0.63(27)	0.84(15)
$p < 0.001$	0.57(134)	0.63(148)	0.66(10)	–(0)

[a]Numbers in parentheses indicate number of averaged correlations. Note that the ~1917–1960 epoch was used to develop the statistical models ("calibration period") and therefore may contain artificial skill; the ~1961–1981 period is independent of model development ("verification period").

search radius used for the process modeling study, the statistical model is constructed by selecting the predictors from monthly values of standardized temperature and precipitation for 16 continuous months, from prior-year June through current growing-season year September. Monthly averages were derived from the same set of daily meteorological station records used in the process modeling study; if more than 3 months of data were missing from a given year, then the entire year was marked as missing. Principal component analysis was used to reduce each resulting set of 32 predictor variables to a smaller number of robust predictors using a 50% cumulative variance criterion. The Akaike information criterion is used to select the most robust regression model. To test the calibration of each statistical model, the most recent one third of the available meteorological data is withheld from statistical calibration for verification purposes; this resulted, on average, in 1917–1960 calibration and 1961–1981 verification periods. Note that the realistic skill of the statistical model can only be assessed via tests in the validation period, which contains data not used to develop the statistical model in the first place. As with the process model simulations described above, the most significant correlation found within the search radius over the full intercomparison period (averaging 1917–1981) is reported. We did not apply and report this approach for the eight Russian data series, because only single nearest meteorological station data were available.

[27] A summary of the statistical modeling results is in Table 3. Scatterplots of the correlation of process model and statistical models with the actual tree-ring width chronologies for annual and decadal averages, and across development and verification periods, are shown in Figure 6; a

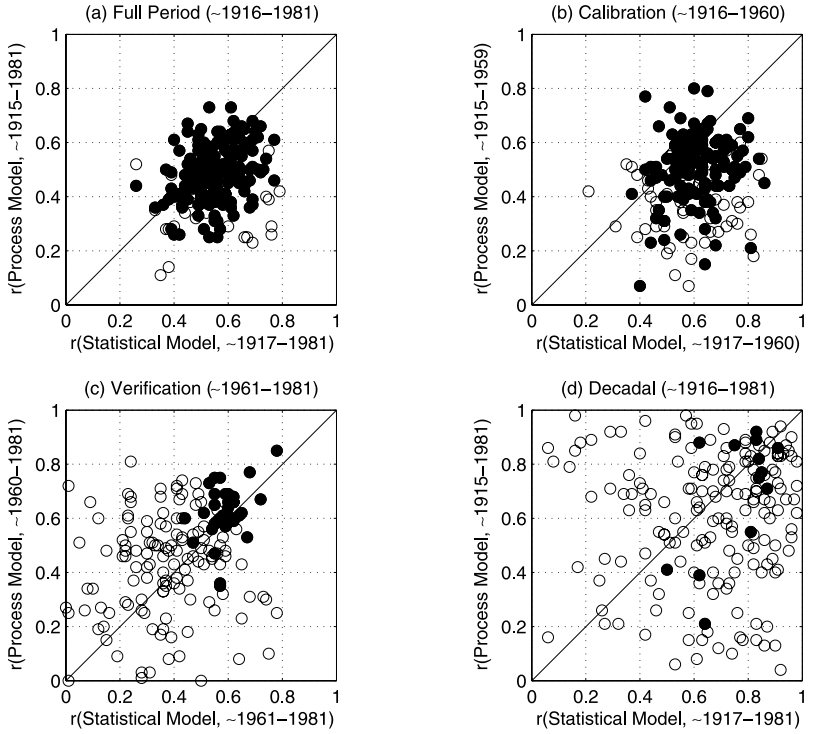

Figure 6. Correlation of the process and statistical model results with actual North American tree-ring chronologies. Correlations are plotted for chronologies for which both successful process and statistical model simulations were made (N = 184; open circles) and for chronologies for which both process model and statistical model correlations reached the 95% confidence level for each intercomparison shown (N varies: see Table 4; solid circles). (a) Process model versus statistical model correlation, annual values, full ~1916–1981 intercomparison period; solid 1:1 line indicates equal model skill. (b) As in Figure 6a, except for ~1916–1960 calibration epoch. (c) As in Figure 6a, except for ~1961–1981 verification period. (d) As in Figure 6a, except for decadal-scale (11-year running mean) correlations.

Table 4. Comparison of Process and Statistical Model Results[a]

	All Comparable Simulations			95% Confidence Level Simulations		
Epoch	Process	Statistical	Number $r_P > r_S$	Process	Statistical	Number $r_P > r_S$
~1916–1981 annual	0.47 ± 0.0087	0.55 ± 0.0078	52(184) ± 6.8	0.49 ± 0.0083	0.56 ± 0.0074	48(161) ± 6.3
~1916–1960 annual	0.46 ± 0.0011	0.60 ± 0.0084	42(184) ± 6.8	0.51 ± 0.011	0.61 ± 0.0087	35(127) ± 5.6
~1961–1981 annual	0.43 ± 0.017	0.37 ± 0.017	109(184) ± 6.8	0.62 ± 0.018	0.59 ± 0.011	23(34) ± 2.9
~1916–1981 decadal	0.61 ± 0.018	0.67 ± 0.016	73(184) ± 6.8	0.69 ± 0.064	0.76 ± 0.035	4(13) ± 1.8

[a]Epochs are averaged across statistical and process epochs for all comparable simulations. Ranges give ±1 standard error in mean correlation values. For 95% confidence level comparisons, numbers in parentheses give number of comparisons. Number $r_p > r_s$, number of correlations for which the process modeling result was better than the statistical modeling result. Theoretical standard errors for $r_p > r_s$ are equal to $\sqrt{N}/2$.

summary of the modeling intercomparison is given in Table 4. The statistical approach was able to define successful models for 184 of the 190 North American chronologies, with an average correlation of 0.55; 181 of 184 chronologies were simulated with an average correlation of 0.55 at the 95% confidence level. Average correlations for calibration and verification epochs are 0.60 and 0.37, respectively (Table 3), revealing significant artificial skill increase during the calibration period, despite our efforts to create robust statistical models. On decadal timescales, the average correlation is 0.67 for all modeled chronologies, and is 0.80 with 56 of 184 chronologies significantly correlated at the 95% level.

[28] An additional way of quantifying the model intercomparison is to ask how often (i.e., in how many locations) the process model produces higher correlations than the statistical model. That is, what is the percentage of points above the 1:1 line in the panels of Figure 6 and is it significantly different from 50%? This comparison of the process and statistical modeling results is presented in Table 4 for all chronologies modeled by both statistical and process modeling approaches, and specifically for only those comparisons by epoch which are at or above the 95% confidence level for a given epoch. Results for the entire period of study (~1916–1981) show that the process and statistical models are each able to explain, on average, about 25–30% of the variance in the tree-ring observations (Figure 6a). In the first epoch (~1916–1960), which is the calibration period for statistical modeling, and for all chronologies modeled by both statistical and process models, the statistical model clearly outperforms the process model (Figure 6b and Table 4), with only 23% of correlations above the 1:1 line. However, some of the statistical modeling skill is likely due to the artificial skill of the statistical models in their calibration period. In the second epoch (~1961–1981), which is the verification period for the statistical model, and is thus free of artificial skill, statistical modeling skill is no different than that of the process model (Figure 6c and Table 4); now 59% of correlations are above the 1:1 line. For just the comparisons that were at or above the 95% confidence level (solid black circles in Figure 6), the correlations of the process and statistical models are indistinguishable within uncertainty.

5. Discussion

5.1. Process Model Skill

[29] We believe process model skill in simulation of tree-ring width chronologies without chronology-specific tuning comes from three major features. First, the model uses realistic, nonlinear functional forms to represent the dependence of trees on soil moisture and temperature (Figure 1). As illustrated for the Ulan-Ude site, the explicit incorporation of the principle of limiting factors permits the model to flexibly respond to multivariate controls on tree growth throughout the year (Figures 1–4). Second, the model incorporates a simple yet effective water balance model that calculates net change in water availability due to runoff, evapotranspiration, and demand (Figure 1). In many locales, this, combined with the modeled predetermination of the number of cambial cells at the start of the growth season, permits effective and realistic intraseasonal switches of the growth-limiting environmental control between temperature and moisture for temperate and subarctic sites (Table 2). Third, the use of daily resolution input data to drive the model permits flexible responses to rapid changes in environmental controls on growth; in particular, it can accurately determine the beginning and end of the growing season (e.g., Figure 2). The generally excellent aggregrate results (Figures 5 and 6 and Tables 2–4) are likely due to these process modeling features.

[30] There are three important sources of uncertainty in the process model simulations. The first of these is that the quality of simulations varies with tree taxon (results not shown); pines, firs and junipers are best simulated by the model; hemlock simulations are poorest. The second is the quality and accuracy of local precipitation data. For example, moisture-stressed Russian tree-ring width chronologies that were successfully simulated using weather station data as model input were not simulated well using NCEP reanalysis data [*Kistler et al.*, 2001] instead of station observations. This is likely to be due to the well-known, poor representation of precipitation on small spatial scales in the NCEP reanalysis [e.g., *Hagemann and Gates*, 2001]. The third is that model parameters were held fixed for all simulations reported this study. However, we have found [*Anchukaitis et al.*, 2006; Vaganov et al., submitted manuscript, 2006] that we can improve simulations of eastern and southeastern U.S. conifers to levels observed in the western United States in this study merely by a priori adjustment of one parameter, the water drainage coefficient Λ (Table 1), to reflect local conditions more accurately.

[31] Given these strengths and weaknesses we are encouraged that the aggregate process model results indicate skill which is roughly equal to that of classical cross-verified statistical modeling techniques (Tables 2–4). For the entire comparison data set (N = 184), we find that the statistical modeling is highly significantly ahead during the ~1916–1981 calibration period, so much so as to also be ahead for the whole period and the decadal averages.

However, the statistical modeling is guaranteed to do well in the calibration period by definition, because the linear regressions are constructed using data from this period. An analogous and equally artificial result would be obtained if we had adjusted the process model's parameters to obtain the best fit for each modeled tree-ring width chronology. The true test of the statistical modeling is in the ~1961–1981 verification period, for which results are independent of statistical model development. In the verification interval, the process modeling skill is about the same as that of the statistical modeling, so the statistical modeling's "wins" in the calibration and full periods likely reflect artificial skill. This interpretation is supported by the skill similarity when only correlations for each epoch significant at or above the 95% level are averaged (Figure 6 and Table 4), although the complete set of 184 statistical modeling results had passed the multiple tests for robust regression described in section 4.4. We feel justified in drawing the weak conclusion that neither method is decisively more skillful in this comparison.

5.2. Model Stability

[32] Results for a range of environments, species, timescales and epochs suggest that the Vaganov-Shashkin process model is capable of simulating a wide variety of tree-ring records and their response to climate forcing, as represented by sunlight, temperature, and precipitation. Experiments exploring a wide range of temperature and water budget parameter space suggest that the model output considered here, ring width index, is not especially sensitive to the choice of these parameters. Rather, the shape of the moisture and temperature growth functions is likely the key element for accurate modeling of the response to moisture availability (Figures 1–4). The generality of the model and its relative insensitivity to tuning parameters are also demonstrated by high correlation with actual tree-ring data from the warm, arid southwest United States; cold, moist Siberia; and to a lesser extent, the warm, moist southeastern United States (Figure 5). We further note that the results shown here do not depend sensitively on meteorological station search radius: average results for 200-km search radii, not shown, were similar to those presented in Figure 5. These results support earlier case studies demonstrating successful application of the VS model for a variety of circumstances [cf. *Vaganov et al.*, 2006, chap. 8, submitted manuscript, 2006].

[33] For the aggregate tree-ring data set studied here, the process model appears to simulate annual and decadal climate variability about as well as standard statistical transfer function methods calibrated on monthly climate data (Tables 2 and 3 and Figure 6). Decadal-scale skill may derive from the predetermination by prior conditions of the number of cambial cells available at the start of the growing season in the simulation model (section 2.4), or it may be due to the nonlinear form of the growth model G. More study is needed to fully characterize the origins of the decadal skill in the process model results. However, process model skill appears to be more temporally stable than that of linear statistical models, whose form and skill may be dependent on the period chosen for its calibration (Tables 2–4 and Figures 6b and 6c). All else being equal, temporal stability of the skill estimate is preferable because it indicates that the estimated skill level is not better than usual just by chance within a limited comparison time interval.

5.3. Implications for Statistical Paleoclimatology

[34] We have shown that a highly simplified but nonlinear forward model produces skillful simulations of a broad network of actual tree-ring width data on interannual to decadal timescales. Although the Vaganov-Shashkin model is a gross representation of the actual complexity of real trees, it is also more complex and closer to biological first principles than the robust linear regressions at the heart of most large-scale paleoclimate field reconstruction activities. An important assumption behind those efforts which depend on tree-ring width chronologies is that the proxy data from this biological archive are linearly related to either local, regional or global patterns of climate variation. The results of this study provide support for this assumption that is not predicated on an assumption of linearity.

[35] This conclusion is especially critical for the interpretation of decadal-scale variations in the tree-ring width data [e.g., *Evans et al.*, 2001; *Cook et al.*, 1999; *Villalba et al.*, 2001], because of the potential for improving annual resolution climate reconstructions for the last millennium. There are many potential sources of decadal-scale variations in tree ring width data, including insect outbreaks, fire ecology, succession, and sampling effects, all of which may or may not have direct links to climate. These cannot be separated from decadal-scale climate variability directly recorded in tree-ring widths by statistical means. The ability of the biologically based process model to successfully simulate the decadal variability observed in the actual tree-ring width data in about a fifth of the simulations (Table 2, 95% significance level results) and in specific cases (e.g., Figure 2) supports their cautious interpretation in terms of climatic variation. That the statistical modeling does similarly well on decadal timescales (Table 3) suggests these models may also be used for robust interpretation as decadal climate indicators in the identified cases. However, in a majority of the tree-ring width chronologies studied here, the decadal variability was not skillfully resolved at or above the 90% level of significance (Tables 2 and 3) by either modeling approach. This suggests that much of the decadal-scale variability evident in the tree-ring width data may not be directly related to decadal-scale climate variations. If this is the case, then improved methods for isolating the true decadal climate signal in the actual tree-ring data should result in similarly improved paleoclimatic reconstructions based on them.

5.4. Future Studies

[36] On the basis of the skill demonstration presented here, there are a number of important applications of the Vaganov-Shashkin model which may be pursued in the future. For instance, the residuals of the fit of the simulated chronologies to the tree-ring width observations could be used to define patterns influencing chronology and/or model error in space, time and frequency. We have shown (Figure 6d) mechanistic support for interpretation of decadal tree-ring variations as climatically driven in a fraction of the tree-ring data set studied here. Hence, in particularly well-observed regions, decadal-scale error functions (corresponding to nonclimatic factors) for tree-ring width

records might be identified. This would represent a significant step toward validating and improving statistically based but ultimately subjective data standardization techniques and identifying decadal climate variability reliably. With the error functions of model and data better resolved, especially on interannual to decadal timescales, we can investigate the inversion of data and model for simultaneous temperature and precipitation reconstructions. GCM output could be used to hindcast probabilistically the natural variability in growth of conifer forest ecosystems and carbon budgets on a global scale. Similarly, climate change forecasts may be transformed into a global conifer forest change "fingerprint" [*Vaganov et al.*, 2006, submitted manuscript, 2006], and the results compared to ongoing satellite observations of the terrestrial ecosystem. These latter applications would require a simulation model expanded to include the effects of changing atmospheric concentrations of carbon dioxide on tree growth.

6. Conclusions

[37] We have found the Vaganov-Shashkin model capable of accurately simulating intraseasonal to interdecadal climate variability, as expressed in variations in tree-ring width, for large regions of North American and Russia. The process model is relatively insensitive to parameter estimation, as shown by the good simulation of actual tree-ring width chronologies from a variety of environments using a single fixed set of model parameters. The overall skill of the process model as applied here is not different from the verification skill of statistical models typically used in dendroclimatology. The ability of the Vaganov-Shashkin model to successfully simulate interannual to decadal scale variations in the observed tree-ring chronologies supports their use as paleoclimatic indicators on these timescales in multivariate climate field reconstruction efforts. The model may be suitable for estimating tree-ring width chronology uncertainty, especially on decadal timescales, constraining paleoclimatic field reconstructions, and assessing the effects of anthropogenic climate change on aspects of the growth of temperate conifer forests.

[38] **Acknowledgments.** The first two authors contributed equally to this work. We thank L. Bengtsson, E. R. Cook, and G. C. Jacoby for their valuable scientific support; A. V. Shashkin, V. V. Shishov, and M. N. Naurzbaev for program code and operational weather station data; and contributors to the International Tree Ring Data Bank of the World Data Center of Paleoclimatology (ITRDB) and the Mann et al. [1998] data set. This study was supported by NOAA grants NA86GP0437 and NA16GP1616 to M. A. C., A. K., M. N. E., and B. K. R., and an Alexander von Humboldt Foundation Feodor Lynen Fellowship to B. K. R. This is LDEO contribution number 6941.

References

Alisov, B. P. (1956), *Climate of the USSR* (in Russian), 126 pp., Moscow State Univ. Publ., Moscow.

Anchukaitis, K. J., M. N. Evans, A. Kaplan, E. A. Vaganov, H. D. Grissino-Mayer, M. K. Hughes, and M. A. Cane (2006), Forward modeling of regional-scale tree-ring patterns in the southeastern United States and the recent influence of summer drought, *Geophys. Res. Lett.*, *33*, L04705, doi:10.1029/2005GL025050.

Andreev, S. G., E. A. Vaganov, M. M. Naurzbaev, and A. K. Tulokhonov (1999), Registration of long-term variations in the atmospheric precipitation, Selenga River runoff, and Lake Baikal level by annual pine tree rings, *Dokl. Acad. Sci. USSR, Earth Sci. Ser., Engl. Transl.*, *368*(7), 1008–1011.

Barber, V. A., G. P. Juday, and B. Finney (2000), Reduced growth of Alaskan white spruce in the twentieth century from temperature-induced drought stress, *Nature*, *405*, 668–673.

Briffa, K. R., F. H. Schweingruber, P. D. Jones, T. J. Osborn, S. G. Shiyatov, and E. A. Vaganov (1998), Reduced sensitivity of recent tree-growth to temperature at high northern latitudes, *Nature*, *391*, 678–682.

Briffa, K. R., T. J. Osborn, F. H. Schweingruber, I. C. Harris, P. D. Jones, S. G. Shiyatov, and E. A. Vaganov (2001), Low-frequency temperature variations from a northern tree-ring density network, *J. Geophys. Res.*, *106*, 2929–2941.

Camerero, J. J., J. Guerrero-Campo, and E. Gutierrez (1998), Tree-ring growth and structure of Pinus uncinata and Pinus sylvestris in the central Spanish Pyrenees, *Arct. Alp. Res.*, *30*(1), 1–10.

Cannell, M. G. R., and R. I. Smith (1986), Climatic warming, spring bud burst, and frost damage of trees, *J. Appl. Ecol.*, *23*, 177–191.

Contributors of the International Tree-Ring Data Bank (2002), World Data Center for Paleoclimatology: Tree rings, NOAA/NGDC Paleoclimatol. Program, Boulder, Colo. (Available at http://www.ngdc.noaa.gov/paleo/treering.html)

Cook, E. R., and L. Kairiukstis (1990), *Methods of Dendrochronology: Applications in the Environmental Sciences*, 394 pp., Springer, New York.

Cook, E. R., D. Meko, D. Stahle, and M. K. Cleaveland (1999), Drought reconstructions for the continental United States, *J. Clim.*, *12*, 1145–1162.

Cook, E. R., R. D. D'Arrigo, and M. E. Mann (2002), A well-verified, multiproxy reconstruction of the winter North Atlantic Oscillation index since AD 1400, *J. Clim.*, *15*, 1754–1764.

Donaldson, J. R., and P. V. Tryon (1987), *User's Guide to STARPAC: The Standards Time Series and Regression Package*, Natl. Inst. of Standards and Technol., Gaithersburg, Md.

Esper, J., E. R. Cook, and F. H. Schweingruber (2002), Low-frequency signals in long tree-ring chronologies for reconstructing past temperature variability, *Science*, *295*, 2250–2253.

Evans, M. N., A. Kaplan, M. A. Cane, and R. Villalba (2001), Globality and optimality in climate field reconstructions from proxy data, in *Interhemispheric Climate Linkages*, edited by V. Markgraf, pp. 53–72, Cambridge Univ. Press, New York.

Foster, J. R., and D. C. LeBlanc (1993), A physiological approach to dendroclimatic modeling of oak radial growth in the midwestern United States, *Can. J. For. Res.*, *23*, 783–798.

Fritts, H. C. (1976), *Tree Rings and Climate*, Elsevier, New York.

Fritts, H. C. (1991), *Reconstructing Large-Scale Climatic Patterns From Tree-Ring Data*, Univ. of Ariz. Press, Tucson.

Fritts, H. C., A. V. Shashkin, and G. M. Downes (1999), A simulation model of conifer ring growth and cell structure, in *Tree-Ring Analysis*, edited by R. Wimmer and R. E. Vetter, pp. 3–32, Cambridge Univ. Press, New York.

Gates, D. M. (1980), *Biophysical Ecology*, 611 pp., Springer, New York.

Graybill, D. A., and S. B. Idso (1993), Detecting the aerial fertilization effects of atmospheric CO_2 enrichment in tree-ring chronologies, *Global Biogeochem. Cycles*, *7*, 81–95.

Gregory, R. A. (1971), Cambial activity in Alaskan white spruce, *Am. J. Bot.*, *58*(2), 160–171.

Guiot, J. (1990), Methods of calibration, in *Methods of Dendrochronology: Applications in the Environmental Sciences*, edited by E. Cook and L. Kairiukstis, pp. 165–178, Springer, New York.

Hagemann, S., and L. D. Gates (2001), Validation of the hydrological cycle of ECMWF and NCEP reanalyses using the MPI hydrological discharge model, *J. Geophys. Res.*, *106*, 1503–1510.

Hanninen, H. (1991), Modeling dormancy release in trees from cool and temperate regions, in *Process Modeling of Forest Growth Responses to Environmental Stress*, edited by R. K. Dixon et al., pp. 159–165, Timber Press, Portland, Oreg.

Jones, P. D., T. J. Osborn, and K. R. Briffa (2001), The evolution of climate over the last millennium, *Science*, *292*, 662–667.

Kirdyanov, A., M. K. Hughes, E. A. Vaganov, F. H. Schweingruber, and P. Silkin (2003), The importance of early summer temperature and date of snow melt for tree growth in the Siberian Subarctic, *Trees*, *17*, 61–69.

Kistler, R., et al. (2001), The NCEP-NCAR 50-year reanalysis: Monthly means CD-ROM and documentation, *Bull. Am. Meteorol. Soc.*, *82*, 247–267.

Kramer, P. J., and T. T. Kozlowski (1979), *Physiology of Woody Plants*, 811 pp., Elsevier, New York.

LaMarche, V. C., D. A. Graybill, H. C. Fritts, and M. R. Rose (1984), Increasing atmospheric carbon dioxide: Tree ring evidence for growth enhancement in natural vegetation, *Science*, *225*, 1019–1021.

Landsberg, J. J. (1974), Apple fruit bud development and growth: Analysis and an empirical model, *Ann. Bot.*, *38*, 1013–1023.

Lindsay, A. A., and J. E. Newman (1956), Uses of official weather data in spring time-temperature analysis of an Indiana phenological record, *Ecology*, *37*, 812–823.

Lyr, H., H. J. Fiedler, and W. Tranquillini (1992), *Physiologie und Ökologie der Gehölze*, 620 pp., Fischer Publ., Jena, Germany.

Mann, M. E., and P. Jones (2003), Global surface temperatures over the past two millennia, *Geophys. Res. Lett.*, *30*(15), 1820, doi:10.1029/2003GL017814.

Mann, M. E., R. S. Bradley, and M. K. Hughes (1998), Global-scale temperature patterns and climate forcing over the past six centuries, *Nature*, *392*, 779–787.

Mann, M. E., R. S. Bradley, and M. K. Hughes (1999), Northern Hemisphere temperatures during the past millennium: Inferences, uncertainties, and limitations, *Geophys. Res. Lett.*, *26*, 759–762.

Mann, M. E., E. Gille, R. S. Bradley, M. K. Hughes, J. T. Overpeck, F. Keimig, and W. Gross (2000), Global temperature patterns in past centuries: An interactive presentation, *Earth Interact.*, *4*(4), 1–29.

Misson, L. (2004), MAIDEN: A model for analyzing ecosystem processes in dendroecology, *Can J. For. Res.*, *34*, 874–887.

Monteith, J. L., and M. H. Unsworth (1990), *Principles of Environmental Physics*, 291 pp., Edward Arnold, London.

Peterson, T. C., and R. S. Vose (1997), An overview of the global historical climatology network temperature data base, *Bull. Am. Meteorol. Soc.*, *78*, 2837–2849.

Schweingruber, F. H. (1988), *Tree-rings: Basics and Applications of Dendrochronology*, D. Reidel, Springer, New York.

Shashkin, A. V., and E. A. Vaganov (1993), Simulation model of climatically determined variability of conifers' annual increment (on the example of common pine in the steppe zone), *Russ. J. Ecol.*, *24*, 275–280.

Stahle, D. W., R. D. D'Arrigo, and P. J. Krusic (1998), Experimental dendroclimatic reconstruction of the Southern Oscillation, *Bull. Am. Meteorol. Soc.*, *79*, 2137–2152.

Thornthwaite, C. W., and J. R. Mather (1955), *The Water Balance*, *Publ. Climatol.*, vol. 1, pp. 1–104, Drexel Inst. of Technol., Philadelphia, Pa.

Trenberth, K. E. (1984), Signal versus noise in the Southern Oscillation, *Mon. Weather Rev.*, *112*, 326–332.

Vaganov, E. A. (1996), Analysis of seasonal growth pattern and modeling in dendrochronology, in *Tree-Rings, Environment and Humanity*, edited by J. S. Dean, D. M. Meko, and T. W. Swetnam, pp. 73–87, Radiocarbon, Tucson, Ariz.

Vaganov, E. A., A. V. Shashkin, and I. V. Sviderskaya (1985), *Histometric Analysis of Woody Plant Growth* (in Russian), 102 pp., Nauka, Novosibirsk, Russia.

Vaganov, E. A., I. V. Sviderskaya, and E. N. Kondratyeva (1990), Climatic conditions and tree ring structure: Simulation model of tracheidogram (in Russian), *Lesovedenie*, *2*, 37–45.

Vaganov, E. A., L. G. Visotskaya, and A. V. Shashkin (1994), Seasonal growth and structure of larch annual rings at the northern timberline (in Russian), *Lesovedenie*, *5*, 3–15.

Vaganov, E. A., M. K. Hughes, A. V. Kirdyanov, F. H. Schweingruber, and P. P. Silkin (1999), Influence of snowfall and melt timing on tree growth in subarctic Eurasia, *Nature*, *400*, 149–151.

Vaganov, E. A., K. R. Briffa, M. N. Naurzbaev, F. H. Schweingruber, S. G. Shiyatov, and V. V. Shishov (2000), Long-term climatic changes in the Arctic region of the Northern Hemisphere, *Dokl. Akad. Sci. USSR, Earth Sci. Ser., Engl. Transl.*, *375*, 1314–1317.

Vaganov, E. A., M. K. Hughes, and A. V. Shashkin (2006), *Growth Dynamics of Tree Rings: Images of Past and Future Environments*, Springer, New York.

Valentine, H. T. (1983), Bud break and leaf growth functions for modeling herbivary in some gypsy moth hosts, *For. Sci.*, *29*, 607–617.

Villalba, R., R. D. D'Arrigo, E. R. Cook, G. Wiles, and G. C. Jacoby (2001), Decadal-scale climatic variability along the extra-tropical western coast of the Americas over past centuries inferred from tree-ring records, in *Interhemispheric Climate Linkages*, edited by V. Markgraf, pp. 155–172, Cambridge Univ. Press, New York.

Wallace, J. M., and P. V. Hobbs (1977), *Atmospheric Science: An Introductory Survey*, 467 pp., Elsevier, New York.

Wang, L., S. Payette, and Y. Bégin (2002), Relationships between anatomical and densitometric characteristics of black spruce and summer temperature at tree line in northern Quebec, *Can. J. For. Res.*, *32*, 477–486.

World Data Center for Paleoclimatology (2003), WebMapper display of tree-ring data sampling sites, http://www.ngdc.noaa.gov/paleo/, Natl. Geophys. Data Cent., Boulder, Colo.

K. J. Anchukaitis, M. N. Evans, and M. K. Hughes, Laboratory of Tree-Ring Research, University of Arizona, Tucson, AZ 85721, USA. (kanchuka@ltrr.arizona.edu; mevans@ltrr.arizona.edu; mhughes@ltrr.arizona.edu)

M. A. Cane and A. Kaplan, Lamont-Doherty Earth Observatory, Columbia University, Palisades, NY 10964, USA. (mcane@ldeo.columbia.edu; alexeyk@ldeo.columbia.edu)

B. K. Reichert, German Meteorological Service, Department FE ZE, Kaiserleistrasse 42, D-63067 Offenbach, Germany. (bernhard.reichert@dwd.de)

E. A. Vaganov, V. N. Sukachev Institute of Forest, Russian Academy of Sciences, Krasnoyarsk, Russia. (eavaganov@forest.akadem.ru)